Spectral diffusion and line broadening in single self-assembled GaAs/AlGaAs quantum dot photoluminescence

M. Abbarchi,[1,a)] F. Troiani,[2] C. Mastrandrea,[1] G. Goldoni,[2] T. Kuroda,[3] T. Mano,[3] K. Sakoda,[3] N. Koguchi,[4] S. Sanguinetti,[4] A. Vinattieri,[1] and M. Gurioli[1]
[1]*European Laboratory for Non-Linear Spectroscopy, and Dipartimento di Fisica, Università di Firenze, Via Sansone 1, 50019 Sesto Fiorentino (Firenze), Italy*
[2]*Istituto Nazionale per la Fisica della Materia (INFM) and Dipartimento di Fisica, Università degli Studi di Modena e Reggio Emilia, Via Campi 213/A, 41100 Modena, Italy*
[3]*National Institute for Materials Science, 1-1 Namiki, Tsukuba, 305-0044, Japan*
[4]*LNESS and Dipartimento di Scienza dei Materiali, Universita di Milano Bicocca, Via Cozzi 53, 120125 Milano, Italy*

(Received 26 June 2008; accepted 26 September 2008; published online 20 October 2008)

We experimentally and theoretically investigate the photoluminescence broadening of different excitonic complexes in single self-assembled GaAs/AlGaAs quantum dots. We demonstrate that the excitonic fine-structure splitting leads to a sizable line broadening whenever the detection is not resolved in polarization. The residual broadening in polarized measurements is systematically larger for the exciton with respect to both the trion and the biexciton recombination. The experimental data agree with calculations of the quantum confined Stark effect induced by charge defects in the quantum dot (QD) environment, denoting the role of the QD spectator carrier rearrangement in reducing the perturbation of the fluctuating environment. © *2008 American Institute of Physics*. [DOI: 10.1063/1.3003578]

Semiconductor quantum dots (QDs)—artificial atoms, as they are often called—share with natural atoms the discrete nature of the electronic energy spectrum. Their engineerable optical excitations, therefore, are ideally suited to coherent carrier control, cavity electrodynamics in the solid state, and quantum-information processing,[1] provided knowledge and control of environmental couplings and decoherence phenomena are achieved.[2] A typical evidence of such environment fluctuations is the inhomogeneous broadening of the photoluminescence (PL) lines of a *single QD*. It is well established that the radiative linewidth of the fundamental excitonic transition in single self-assembled QDs is of a few μeV at cryogenic temperature, while in micro-PL (μPL) experiments values up to hundreds of μeV are observed. The origin of the broadening is known as *spectral diffusion* (SD) and is commonly attributed to the charging and discharging of trap defects on time scales shorter than the long integration time required for a μPL measurement, which results in a time-fluctuating quantum confined Stark effect.[3–6] Moreover, in the presence of SD, one can observe counterintuitive effects, such as the onset of a motional-narrowing regime at low temperatures and excitation powers.[7]

Most experimental studies addressing spectral broadening are performed with unpolarized light. However, typically, in self-assembled QDs excitonic emission shows a fine-structure splitting (FSS),[8–10] coming from partial polarization anisotropy. Since the splitting ($\sim$100 μeV) is typically comparable to the line broadening, *the intrinsic SD contribution to the linewidth of excitonic recombination can only be isolated with polarization-sensitive detection*.

In this letter we report a joint experimental and theoretical study of the line broadening induced by SD in single GaAs/AlGaAs self-assembled QDs. High-resolution, polarization-resolved spectroscopy is employed to characterize the linewidth of excitons (X), biexcitons (XX), and trions (T). Their respective linewidths [reported as full width at half maximum (FWHM)], σ_X, σ_{XX}, and σ_T, show a systematic relationship, with σ_X typically larger than σ_{XX}, and $\sigma_{XX} \simeq \sigma_T$ Theoretical simulations of the Stark shift induced by charged traps account for the observed SD-induced linewidth and provide information on the trap type and localization.

The GaAs/$Al_{0.3}Ga_{0.7}$As QD sample was grown by droplet epitaxy,[11,12] and then annealed at 680 °C for 1 h.[11] The QDs are lens shaped, with radius typically ranging between 5 and 13 nm and an aspect ratio between height h and radius r of $h/r \approx 1.2$. The QD density is $\sim 6 \times 10^8$ QDs/cm^2. The sample was cooled down to cryogenic temperature (T = 20 K) in a low vibration cold finger cryostat and was photoexcited above the AlGaAs barrier energy by a solid state laser emitting at 532 nm. The single QD PL was collected by using a diffraction limited confocal microscope, with a 100× objective (numerical aperture=0.7) and a 5 μm single-mode optical fiber acting as confocal pinhole (lateral resolution of $\sim$0.5 μm). The PL was dispersed through a 1 m focal length, double-grating monochromator and detected by a silicon-based charge coupled device camera. The spectral resolution, as measured by the FWHM of the laser line, was 25 μeV; it allowed to measure line shift as small as 5 μeV. The polarization-dependent FSS was measured by using a linear polarizer and a rotating half-wave plate.

The QD PL spectra are generally characterized by the presence of three main peaks, which are associated with X, T, and XX recombinations, on the ground of intensity-correlation measurements (not shown)[13] and of the FSS analysis. We attribute T to positively charged trions (X^+) due to the slight residual p doping of the structure. Three typical emission lines are shown in Fig. 1(a). The PL linearly polar-

a)Author to whom correspondence should be addressed. Electronic mail: abbarchi@fi.infn.it.

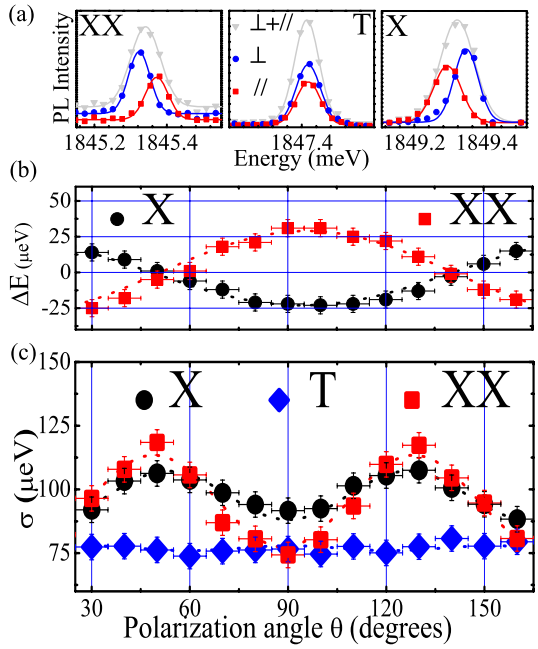

FIG. 1. (Color online) (a) PL lines arising from the *X*, *T*, and *XX* recombinations. Red squares (blue circles) correspond to linearly polarized emission along the [110] ([1$\bar{1}$0]); gray triangles represent the sum of the two. Symbols: experimental data. Lines: Gaussian fit. (b) Black circles and red squares give the positions of the *X* and *XX* peaks as a function of the linear polarization. Dotted lines: sinusoidal fit of the data. (c) Black circles, blue diamonds, and red squares are the line broadenings σ_X, σ_T, and σ_{XX}. Dotted lines: sinusoidal fit of the data.

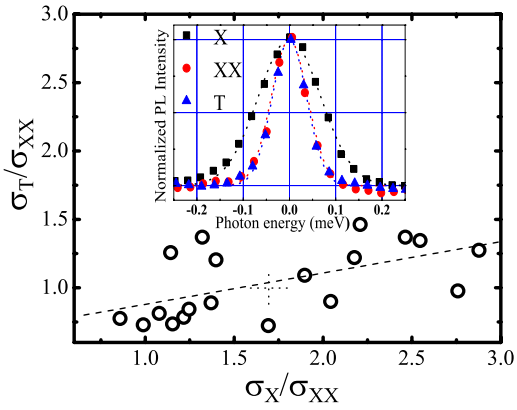

FIG. 2. (Color online) Distribution of the ratio σ_T/σ_{XX} as a function of σ_X/σ_{XX}. The line is a linear fit of the points and the cross represents the average value. Inset: comparison between typical *X* (black squares), *T* (blue triangles), and *XX* (red circles) lines. Symbols: experimental data. Lines: Gaussian fit. The peaks are shifted in frequency and renormalized in intensity in order to make the comparison easier.

ized along the asymmetry axes of the QDs is denoted as $\perp$ (blue circles) and $\parallel$ (red squares) respectively, while the sum of the two is denoted as $\perp+\parallel$ (gray triangles). The *X* and *XX* lines clearly show symmetric polarization splittings, while the *T* emission is polarization independent. It is clear from Fig. 1(a) that the broadening of the total PL ($\perp+\parallel$) of the *X* and *XX* lines is almost twice than that observed when selecting the polarization along one of the asymmetry axes. In order to precisely evaluate this effect, we have studied the FSS of *X*, *T*, and *XX* as a function of the polarization angle. As expected, the linewidths of *XX* and *X* show a clear sinusoidal dependence on the polarization angle (θ), with a periodicity which is twice that of the corresponding FSS. This demonstrates that, besides SD, the presence of FSS in the excitonic emission gives rise to a sizable broadening in the unpolarized QD emission spectra. In the following we analyze the linewidth corresponding to linear polarization along one of the asymmetry axes of the QD (θ=90°).

We have measured the PL from several QDs, emitting at different energies in the spectral interval 1.7–1.9 eV. The *XX* and *T* binding energies usually vary between 3 and 4 meV and 0.7 and 2 meV, respectively, whereas the SD-induced line broadening varies between tens and hundreds of μeV. We find no correlation between linewidth and dot size (i.e., the emission energy), which suggests the extrinsic origin of the line broadening. Analyzing each emission (see Fig. 2), we find instead a clear correlation between the line broadening and the number of carriers in the dot. In particular, it results that σ_X is systematically larger than σ_{XX} and σ_T, which are instead very similar to each other: $\sigma_X > \sigma_T \simeq \sigma_{XX}$. A typical example is shown in the inset of Fig. 2, where the three lines are shifted in energy and renormalized in intensity so as to allow a direct comparison of their broadenings. Averaging the line broadening for each emission we obtain $\bar{\sigma}_X$ =140 μeV, $\bar{\sigma}_T$=92 μeV, and $\bar{\sigma}_{XX}$=87 μeV (cross in Fig. 2). According to previous findings[3–6] we attribute the PL line broadening to SD due to the population of extrinsic levels in the barrier region around the QDs, likely associated with crystalline defects.

In order to understand the observed correlation between the σ values, we calculate the *X*, *XX*, and *T* energy shifts induced by charged traps in the surroundings of the dot. For a given trap position, we first calculate the single-particle states by solving the three-dimensional Schrödinger equation within a single-band effective-mass approximation. In our model, the confinement potential $V_{\mathrm{BO}}^{(\chi)}(\mathbf{r})$ [$\chi=e,h$ identifies the electron (e) and hole (h) states in the QD] is provided by the band offset between a disk-shaped GaAs region and a surrounding $Al_{0.3}Ga_{0.7}As$ barrier: $V_{\mathrm{BO}}^{(\chi)}(\rho,z)=0$ for $0<\rho<r$ and $0<|z|<h/2$ and $V_{\mathrm{BO}}^{(\chi)}(\rho,z)=V_0^{(\chi)}>0$ elsewhere. The presence of a trapped charge in the surroundings of the dot results in an additional contribution to the potential $V^{(\chi)}(\mathbf{r})=V_{\mathrm{BO}}^{(\chi)}(\mathbf{r})+q/\epsilon|\mathbf{r}-\mathbf{R}|$, ϵ being the bulk dielectric constant. We then compute the energies of *X* and *XX* and positively or negatively charged trions, $T=X^{\pm}$, by diagonalizing the few-particle Hamiltonian $H=\Sigma_\chi H_{\mathrm{SP}}^{(\chi)}+\Sigma_{\chi,\chi'} H_C^{(\chi\chi')}$, where $H_{\mathrm{SP}}^{(\chi)}$ and $H_C^{(\chi\chi')}$ are the single-particle and (intradot) Coulomb interaction terms, respectively.[14] Finally, we identify the optical transitions between the ith eigenstate $|\Psi_i^\alpha\rangle$ of the electron-hole complex $\alpha=X,X^+,X^-,XX$ and the jth eigenstate $|\Psi_j^\beta\rangle$ of $\beta(\alpha)=vac,h,e,X$, respectively. In the following, we focus on transitions between ground states ($i=j=0$), whose transition energy is ϵ^α. The quantity to be compared with the inhomogeneous broadening σ is the shift in the optical transitions induced by a charge q trapped at different positions $\mathbf{R}$ from the QD. This is given by the difference between the Stark shifts of the initial and final states, $\Delta\epsilon^\alpha(\mathbf{R})=\Delta E_0^\alpha(\mathbf{R})-\Delta E_0^{\beta(\alpha)}(\mathbf{R})$. Assuming singly charged traps, we have calculated the spectral shifts for four possible scenarios, with positive/negative charge $q=\pm|e|$ and traps localized in the plane of the QD or along the growth direction $\hat{z}$.

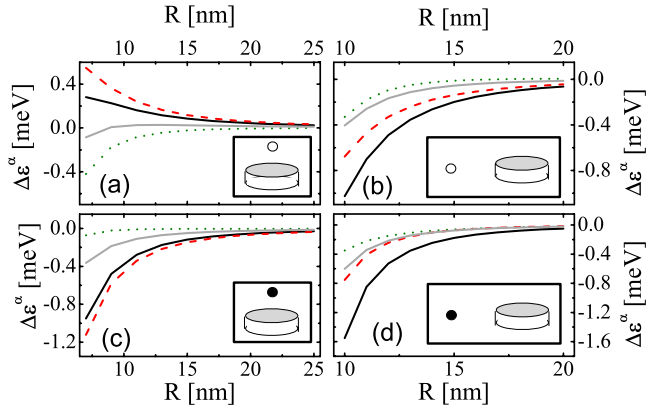

FIG. 3. (Color online) Calculated energy shift of the optical transitions of X, XX, and $T=X^{\pm}$ of a disk-shaped QD resulting from the presence of holes [$q=+|e|$, panels (a) and (b)] or electrons [$q=-|e|$, (c) and (d)] trapped in its surroundings. The dot height and radius are given by $r=5$ nm and $h=8$ nm. The trapped carrier is positioned at a distance $\mathbf{R}$ from the disk center, either along its symmetry axis z [$\mathbf{R}\|\hat{z}$, panels (a) and (c)] or in the plane [$\mathbf{R}\perp\hat{z}$, panels (b) and (d)], as indicated in the insets. The initial electron-hole complex α corresponds to X (solid black lines), X^{+} (dotted green), X^{-} (dashed red), and XX (solid gray).

The results are shown in Fig. 3 for a disk-shaped model QD, with dimensions and interlevel spacings corresponding to a typicaly observed dot (see caption). Quite remarkably, different charge signs and positions of the traps give rise to qualitatively different behaviors, which are found to be rather robust with respect to the QD shape and size (not shown here). In general, the energy shifts corresponding to $\mathbf{R}\perp\hat{z}$ are larger than those for $\mathbf{R}\|\hat{z}$, because the in-plane confinement here is weaker than the one in the growth direction. The generally obtained negative shifts of the optical transition correspond to the electron-hole complexes, α being more redshifted (less blueshifted) than the corresponding β. More specifically, we find that the ratios $\Delta\epsilon^{\alpha}/\Delta\epsilon^{\alpha'}$ are incompatible with the observed ratios between the corresponding broadenings, $\sigma_{\alpha}/\sigma_{\alpha'}$, if the trapped carriers are holes localized on top of the dot [panel (a)]. Qualitative agreement between theory and experiment is found for panels (b)–(d). In particular, the calculated ratios are in good agreement with the average measured ratios when the quantum confined Stark shift is induced by electrons in the plane [panel (d)]. We finally note that the dependence of the Stark shifts $\Delta\epsilon_i^{\alpha}$ on the field induced by the trap is cubic for all the considered optical transitions from trion states, $\Delta\epsilon^{X^{\pm}}$.

In conclusion, we have performed high-resolution polarization-resolved μPL spectroscopy of single GaAs/AlGaAs self-assembled QDs to highlight the contribution of SD to the linewidth of excitons, biexcitons, and trions. We find systematic relationships with the X linewidth typically larger than the XX and T linewidths, reflecting the different degrees of polarizability of X, XX, and T states. Theoretical investigation shows that the spectral shift of the different excitonic complexes are specific of the sign/localization of the traps. Therefore, the SD-induced linewidth of μPL contains detailed information on the nature and localization of the traps.

This work was supported by Program No. RBIN06JB4C, MIUR-FIRB No. RBIN04EY74, and PRIN 2006 No. 2006022932.

[1] D. D. Awschalom, D. Loss, and N. Samarth, in *Semiconductor Spintronics and Quantum Computation* (Springer, Berlin, 2002).
[2] F. Troiani, U. Hohenester, and E. Molinari, Phys. Rev. B **62**, R2263 (2000).
[3] S. A. Empedocles, D. J. Norris, and M. G. Bawendi, Phys. Rev. Lett. **77**, 3873 (1996).
[4] H. D. Robinson, B. B. Goldberg, L. Marsal, and H. Mariette, Phys. Rev. B **61**, R5086 (2000).
[5] L. Besombes, K. Kheng, L. Marsal, and H. Mariette, Phys. Rev. B **65**, 121314 (2002).
[6] I. Favero, A. Berthelot, G. Cassabois, C. Voisin, C. Delalande, P. Roussignol, R. Ferreira, and J. M. Gerard, Phys. Rev. B **75**, 073308 (2007).
[7] A. Berthelot, I. Favero, G. Cassabois, C. Voisin, C. Delalande, P. Roussignol, R. Ferreira, and J. M. Gerard, Nat. Phys. **2**, 759 (2006).
[8] M. Sugisaki, H.-W. Ren, S. V. Nair, K. Nishi, S. Sugou, T. Okuno, and Y. Masumoto, Phys. Rev. B **59**, R5300 (1999).
[9] M. Bayer, A. Kuther, A. Forchel, A. Gorbunov, V. B. Timofeev, F. Schäfer, J. P. Reithmaier, T. L. Reinecke, and S. N. Walck, Phys. Rev. Lett. **82**, 1748 (1999).
[10] G. Bester, S. Nair, and A. Zunger, Phys. Rev. B **67**, 161306 (2003).
[11] V. Mantovani, S. Sanguinetti, M. Guzzi, E. Grilli, M. Gurioli, K. Watanabe, and K. Koguchi, J. Appl. Phys. **96**, 4416 (2004).
[12] T. Mano and N. Koguchi, J. Cryst. Growth **278**, 108 (2005).
[13] T. Kuroda, M. Abbarchi, T. Mano, K. Watanabe, M. Yamagiwa, K. Kuroda, K. Sakoda, G. Kido, N. Koguchi, C. Mastrandrea, L. Cavigli, M. Gurioli, Y. Ogawa, and F. Minami, Appl. Phys. Express **1**, 042001 (2008).
[14] D. Bellucci, F. Troiani, G. Goldoni, and E. Molinari, Phys. Rev. B **70**, 205332 (2004).